International Journal of Mechanical, Industrial and Aerospace Sciences
ISSN: 2517-9950
Vol:10, No:5, 2016

Near Field Focusing Behaviour of Airborne Ultrasonic Phased Arrays Influenced by Airflows

D. Sun, T. F. Lu, A. Zander, M. Trinkle

***Abstract*—**This paper investigates the potential use of airborne ultrasonic phased arrays for imaging in outdoor environments as a means of overcoming the limitations experienced by kinect sensors, which may fail to work in the outdoor environments due to the oversaturation of the infrared photo diodes. Ultrasonic phased arrays have been well studied for static media, yet there appears to be no comparable examination in the literature of the impact of a flowing medium on the focusing behaviour of near field focused ultrasonic arrays. This paper presents a method for predicting the sound pressure fields produced by a single ultrasound element or an ultrasonic phased array influenced by airflows. The approach can be used to determine the actual focal point location of an array exposed in a known flow field. From the presented simulation results based upon this model, it can be concluded that uniform flows in the direction orthogonal to the acoustic propagation have a noticeable influence on the sound pressure field, which is reflected in the twisting of the steering angle of the array. Uniform flows in the same direction as the acoustic propagation have negligible influence on the array. For an array impacted by a turbulent flow, determining the location of the focused sound field becomes difficult due to the irregularity and continuously changing direction and the speed of the turbulent flow. In some circumstances, ultrasonic phased arrays impacted by turbulent flows may not be capable of producing a focused sound field.

***Keywords*—**Airborne, airflow, focused sound field, ultrasonic phased array.

I. Introduction

MACHINE vision is widely applied in the field of agriculture including weed detection [1], automatic fruit picking [2] and livestock identification [3]. In certain agricultural environments, three dimensional imaging has advantages over two dimensional imaging. For instance, in vineyards, the depth information provided by 3-D images permits the targeted row of grapevines to be easily distinguished from the background. Recently, Kinect sensors have been commonly used to generate

3-D images due to their fast processing speed and high accuracy [4]. However, these sensors cannot be successfully applied in an outdoor environment due to the oversaturation of the infrared photo diodes caused by the influence of strong sunlight [4]. To overcome this barrier, one possible approach is to replace Kinect sensors with ultrasonic phased arrays to produce 3-D images, as they are relatively robust against the optical interference.

Phased arrays have been investigated since the late 1950s [5]. The directivity of the arrays in the far-field can be modelled through beam steering algorithms that assume plane wave approximation, where the array elements are considered as monopole sources. This approach has been used for the investigation of the beam properties of many array applications including radiotelescopes [6], radar [7], and GPS [8]. Nevertheless, the plane wave assumption fails in the study of near field focusing behaviour of ultrasonic phased arrays because in the near field spherical wave propagation should be considered, and the dimensions of the array elements must also be taken into account. Wooh and Shi developed such an approach to describe the focusing behaviour using Huygens' Principle in the frequency domain [9]. In the model proposed by Wooh and Shi, the width of the elements was considered, while the elevation dimension was not taken into account [9]. This aspect can be tackled through a modelling method involving time-dependent velocity potential stated by the Rayleigh Equation [10]. The model introduced by Ullate and Emeterio is based on the impulse-convolution response approach [10]. Through this modelling method, the sound pressure distribution due to a single finite size source of arbitrary shape can be simulated. This method was extended by Neild et al. to the simulation of phased arrays [11].

Although the directivity of ultrasonic phased arrays has been well researched for static media [9], [12], there appears to be no comparable examination in the literature of the impact of a flowing medium on the focusing behaviour of near field focused ultrasonic arrays. Recent papers on ultrasonic arrays show that a static medium is commonly used as a precondition of the studies, whereas a flowing medium received little attention [13], [14]. In addition, the impact of wind has not been considered in studies of airborne ultrasonic arrays [9]-[11]. In an underwater environment, the flowing medium has negligible influence on the near field focusing behaviour of ultrasonic arrays, as the velocity of the flow is usually sufficiently slow in comparison to the speed of the sound propagation in water. However, the impact may not be ignored for airborne ultrasonic phased arrays, because the relative velocity of the flow could be considerable in air. Hence, this paper presents a method of modelling the sound pressure field from a focused array influenced by a flow under the condition that the properties of the flow are known. This is an extension of the method for predicting the pressure field from an ultrasonic array in a static propagation medium using the impulse response method [11]. The remainder of this paper is organised as follows: Section II

D. Sun (PhD student), T. F. Lu (Senior Lecturer) and A. Zander (Associate Professor) are with the School of Mechanical Engineering, University of Adelaide, Adelaide, South Australia, Australia (e-mail: d.sun@adelaide.edu.au, tien-fu.lu@adelaide.edu.au, anthony.zander@adelaide.edu.au).

M. Trinkle is in the School of Electrical and Electronic Engineering, University of Adelaide, Adelaide, South Australia, Australia (e-mail: mtrinkle@eleceng.adelaide.edu.au).

presents the theoretical analysis for the pressure fields of focused phased arrays impacted by a flow. The simulation results obtained using this model are presented in Section III. Section IV provides the conclusion of this paper.

II. Analysis of the Focusing Behaviour of Phased Arrays Impacted by Flows

In this section, the analytical modelling of the sound pressure distribution of a single circular source element is introduced, followed by the incorporation of appropriate time delays between the array elements to achieve near field focusing. In addition, the methods simulation used to study the focusing behaviour of an array impacted by uniform flows and turbulence flows are discussed.

A. Sound Pressure Field of a Single Element of Circular Shape

The sound pressure distribution produced by a single ultrasound element of arbitrary shape can be modelled through the impulse response method proposed by Ullate and Emeterio [10]. The approach assumes that the propagation medium of the ultrasound signals is homogeneous and non-dissipative. According to the wave propagation equation, the sound pressure at an arbitrary spatial point, $p(\vec{r},t)$, can be stated as [10].

$$p(\vec{r},t) = \rho\partial\phi(\vec{r},t)/\partial t, \tag{1}$$

where ρ is the density of the propagation medium, $\vec{r}$ is the vector which denotes the spatial location of the point, and ϕ is the time-dependent velocity potential at the spatial point at time t. Fig. 1 shows the geometry and system of coordinates for the impulse response of a circular source element. The surface of the circular element is located on the x-y plane. P' is the projection of the observation point P on the x-y plane. For easier understanding, the circle whose centre is P' with radius r will be named as Circle P', and the sphere whose centre is P with radius R will be named as Sphere P. Circle P' is the cross circle between Sphere P and the x-y plane. Based upon the Rayleigh Equation, ϕ can be expressed as [10].

$$\phi(\vec{r},t) = \int_s v(t - R/c)/2\pi R\, ds, \tag{2}$$

where v is the normal component of the velocity over the surface of the element, and R is the distance from the spatial point to the element area, ds, located on the surface of the source.

Using convolution operator of the Dirac delta function, considering $p(\vec{r},t)$ as the output of the system, (1) can be expressed as [10]

$$p(\vec{r},t) = \rho\partial[v(t) * h(\vec{r},t)]/\partial t, \tag{3}$$

where $v(t)$ is considered as the input of the system, and denotes the waveform of the velocity at the surface of the ultrasound source. $h(\vec{r},t)$ is the impulse response of the system which can be stated as [10]

$$h(\vec{r},t) = \int_s \delta(t - R/c)/\,2\pi R\, ds, \tag{4}$$

which can be further derived as [10]

$$h(\vec{r},t) = c\Omega(\vec{r},t)/2\pi, \tag{5}$$

where $\Omega(\vec{r},t)$ is the angle subtended at P', by the arc intersected by Circle P' and the edge of the ultrasound source element.

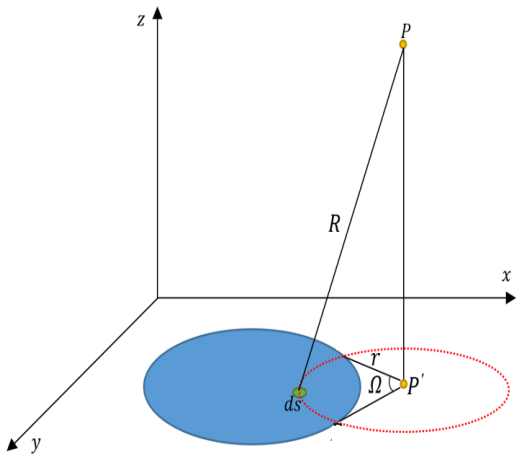

Fig. 1 Geometry and System of Coordinates for the Impulse Response of a Circular Source Element

The angle function $\Omega(\vec{r},t)$ varies for source elements of different shape. Here the function related with a circular ultrasound element is studied as a common shape of ultrasound sensors. For a circular element, $\Omega(\vec{r},t)$ can be analysed for three different distinct regions.

1. Circular Element Region 1: P' Located Outside the Ultrasound Element

Assuming at moment t_1, the edge of Circle P' is tangent to the edge of the element, and at moment t_2 the element is just fully included by Circle P', $\Omega(\vec{r},t)$ can be described as

$$\Omega(\vec{r},t)=\begin{cases}0, & 0 \le t \le t_1\\ \angle AP'B, & t_1 < t < t_2\\ 0, & t \ge t_2\end{cases}, \tag{6}$$

2. Circular Element Region 2: P' Located on the Element Surface and Does Not Overlap the Centre of the Element

Assuming t_1 is the moment when Sphere P is tangent to the surface of the element, t_2 is the moment when Circle P' is tangent to the edge of the element from inside, t_3 is the moment when the element is just fully included by Circle P', $\Omega(\vec{r},t)$ can be described as

$$\Omega(\vec{r},t)=\begin{cases}0, & 0 \le t \le t_1\\ 2\pi, & t_1 < t \le t_2\\ \angle AP'B, & t_2 < t < t_3\\ 0, & t \ge t_3\end{cases}, \tag{7}$$

3. Circular Element Region 3: P' Overlaps the Centre of the Element

$$\Omega(\vec{r},t)=\begin{cases}0, & 0 \le t \le t_1\\ 2\pi, & t_1 < t \le t_2\\ 0, & t > t_2\end{cases}, \quad (8)$$

B. Time Delay Calculation for Near Field Focused Phased Arrays

In order to create a focused field using a phased array, the emitted ultrasound waves from each of the array elements must arrive at the focal point in phase. To achieve this, a time shift is applied to the elements [7]. For arrays focused in the far field, the dimension of the array can be neglected, thus the distance from each array element to the focal point is considered as approximately equal. This approximation is not appropriate for calculation of the time delays for near field focused arrays, because in the near field, the dimension of the array must be taken into account. As a result, Neild et al. proposed an approach for calculating the firing time differences among the array elements, which is named as the time advance method [10]. Through this approach, the error caused by the far field approximation can be eliminated.

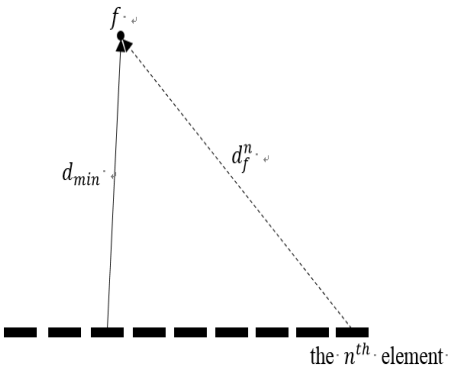

Fig. 2 Geometry schematic diagram of time-shift pattern of a near field focused array

As shown in Fig. 2, the shortest distance from the centre of an element to the focal point is d_{min} and the distance from the centre of the n^{th} element to the focal point is d_f^n, the time advance of the n^{th} element can be calculated as

$$\Delta t^n = (d_f^n - d_f^n - d_{min})/c \quad (9)$$

C. Sound Pressure Field of a Phased Array in a Flow

In the method proposed by Neild et al. [10], the sound pressure field of a phased array is analysed in the spatial coordinate system established on the surface of the array elements, while the observation point is static relating to the array elements. It is inefficient to analyse the impact of a flow on the sound pressure field of the array in this coordinate system, as the flow has differing influence on the ultrasound signals propagating in different directions. An efficient approach is for the coordinate system to move with the flow, whereby the coordinate system and the spatial observation point move in the same direction and at the same speed as the flow, while the array elements remain static. Conversely, it can also be considered that the coordinate system and the spatial observation point remain static, while the array elements move at the same speed of the flow, but in the opposite direction.

Let T denote a period of time, where $T = [t_1, t_2 \dots t_n \dots t_m]$. When a phased array element is exposed to a uniform flow, whose velocity is $v_{uniform}$ and direction as shown in Fig. 3, the location of the centre of the element $[x_n, y_n, z_n]$ at the moment t_n can be calculated by

$$\begin{cases} x_n = x_1 + t_n v_{uniform}\, t_n cos\beta cos\,\alpha \\ y_n = y_1 + t_n v_{uniform} cos\beta\, sin\,\alpha \\ z_n = z_1 - t_n v_{uniform}\, sin\,\beta \end{cases}, \quad (10)$$

where $[x_1, y_1, z_1]$ denote the original location of the centre in the coordinate systems, α and β are the azimuth angle and the elevation angle of the uniform flow.

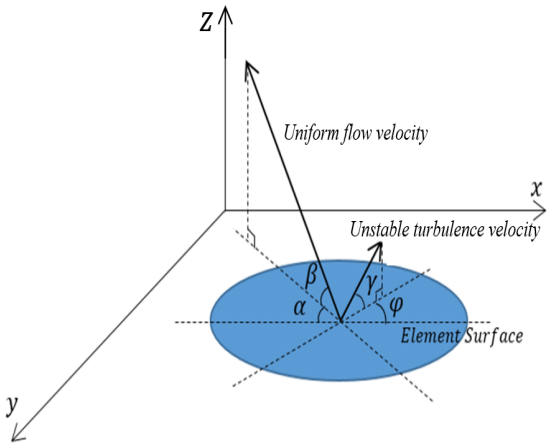

Fig. 3 Flow direction analysis for the modelling of the sound pressure field from a circular source element

When the array element is exposed to a flow which is a combination of a steady uniform flow and a turbulent velocity fluctuation, the velocity of the flow at an instant can be described as [15]

$$\overrightarrow{v_{mix}} = \overrightarrow{v_{uniform}} + \overrightarrow{v_{impulse}}, \quad (11)$$

where $\overrightarrow{v_{impulse}}$ denotes the velocity fluctuation of the turbulent flow at that instant. Assuming the direction of the turbulent flow at the moment t_n is shown as in Fig. 3, the location of the centre at the moment t_n is given by

$$\begin{cases} x_n = x_{n-1} + \Delta t\left(v_{uniform} cos\beta cos\alpha - v_{impulse} cos\varphi cos\gamma\right) \\ y_n = y_{n-1} + \Delta t\left(v_{uniform} cos\beta sin\alpha - v_{impulse} cos\varphi sin\gamma\right) \\ z_n = z_{n-1} - \Delta t\left(v_{uniform}\, sin\,\beta - v_{impulse}\, sin\,\gamma\right) \end{cases} \quad (12)$$

where $\Delta t = t_n - t_{n-1}$.

The developed model for airborne ultrasonic phased arrays influenced by airflows is applied in Section III.

III. Simulation Results and Related Discussion

In this section, the impact of an airflow on a single ultrasound element and on phased arrays are presented and analysed.

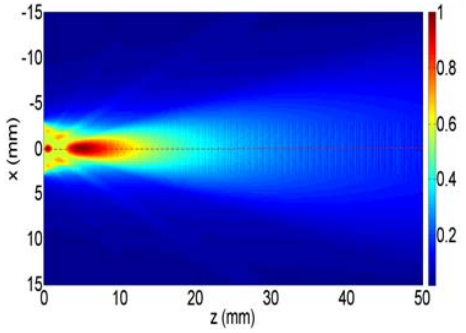

Fig. 4 Predicted peak-to-peak linear sound pressure field normalised to the max pressure in the field in air from a single 3mm diameter circular source driven by a 200 kHz signal

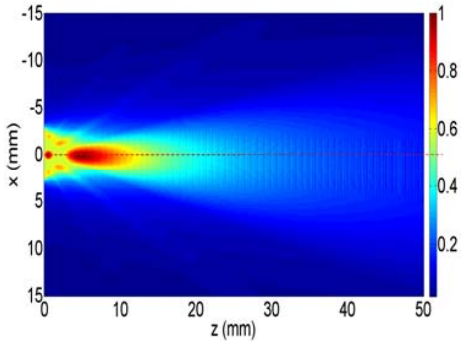

(a)

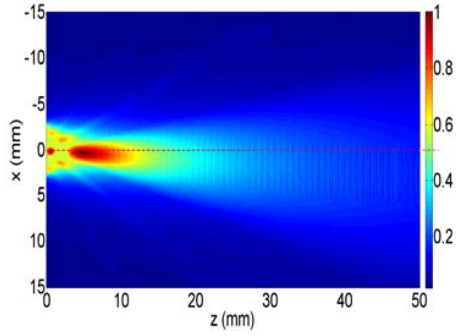

(b)

Fig. 5 Predicted peak-to-peak linear sound pressure field normalised to the max pressure in the field in air from a single 3mm diameter circular source driven by a 200 kHz signal, impacted by a uniform airflow flowing along the positive direction of the *x* axis at a speed of 10 m/s (a) and 20 m/s (b)

A. Impact of an Airflow on a Single Airborne Ultrasound Source Element

Fig. 4 presents predictions of the model for the peak-to-peak sound pressure field normalised to the max pressure in the field for a single circular air-coupled ultrasound source element. The diameter of the element is 3mm and its centre is located on the origin of the coordinate system. Considering the desired balance between desired spatial resolution of the imaging and attenuation in air [16], the driving frequency of the source element was chosen as 200 kHz. In Fig. 4, the spherical spreading of the ultrasound signal is along the positive direction of the z axis. The main lobe and the side lobes are evident.

Fig. 5 shows the predicted sound pressures field of the same element, but impacted by uniform airflows in the positive direction of the x axis. Referring to the angles defined in Fig. 3, the direction of the uniform airflows can be defined as $\alpha = \pi, \beta = 0$. In Australia, the average wind speed in continental area is around 8m/s, and the gusts of 22m/s occur frequently [17]. Thus the speeds of the flows are set to be 10m/s and 20m/s respectively. From comparison of Figs. 4 and 5, it can be seen that when the uniform airflow is flowing along the vertical direction of the spherical spreading, the influence is mainly reflected in the twisting of the emitting angle of the element. As the element is of circular shape, the flow in the direction, which can be defined as $\alpha = -\pi/2, \beta = 0$, has similar impact on the sound pressure field of the element in the y-z plane. The related figures are not presented in this paper.

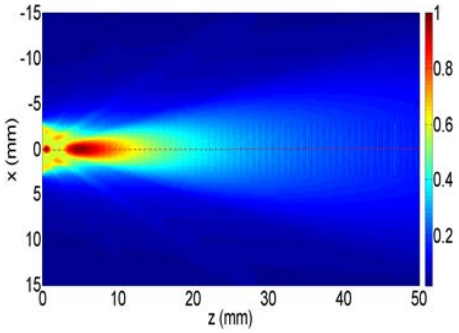

(a)

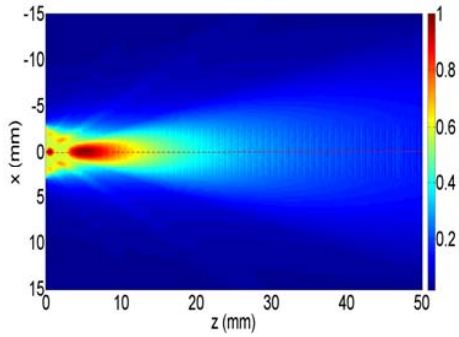

(b)

Fig. 6 Predicted peak-to-peak linear sound pressure field normalised to the max pressure in the field in air from a single 3mm diameter circular source driven by a 200 kHz signal, impacted by a uniform airflow flowing along the positive (a) and negative (b) direction of the z axis at a speed of 20 m/s

Fig. 6 presents the predicted sound pressure field of the same element as presented in Fig. 4, but impacted by uniform

airflows in the direction along the positive and negative directions of the z axis ($\beta = \pi/2, -\pi/2$), at a speed of 20m/s. The simulation results indicate that uniform airflows along the emitting direction of the source element have negligible impacts on the sound pressure distribution of the element. This is because the majority of the sound energy is propagating in the same direction as the airflow, hence the main impact of the flow is reflected in a change in the propagation speed rather than the propagation direction of the sound energy. In most agricultural environments, the wind speed is significantly lower than the speed of sound in air. Therefore, it can be approximately deduced that uniform airflows whose direction is the same as or opposite to the emitting direction of the element have negligible impact on the pressure field of the ultrasound element. Thus, the flows in the directions along the z axis (both positive and negative) are not discussed further in this paper.

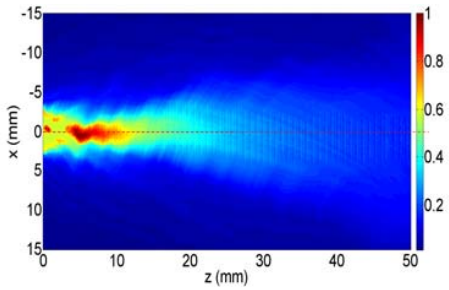

(a)

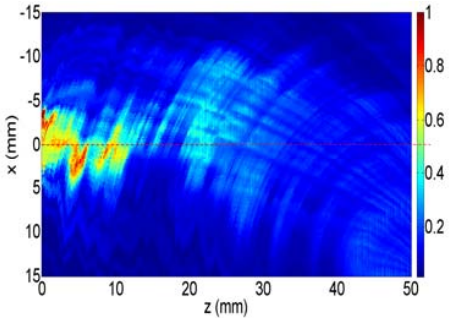

(b)

Fig. 7 Predicted peak-to-peak linear sound pressure field normalised to the max pressure in the field in air from a single 3mm diameter circular source driven by a 200 kHz signal, impacted by a combination of uniform and turbulent airflows. The uniform flow is flowing along the positive direction of the x axis at a speed of 5 m/s, and the velocity fluctuation of the turbulent flow is 1% (a) and 5% (b) of the uniform flow

Fig. 7 illustrates the pressure field of the same element as presented in Fig. 4, but influenced by a combination of uniform and turbulent airflows. The direction of the uniform flow is in the positive direction of the x axis ($\alpha = \pi, \beta = 0$), while the velocity of the uniform flow is 5m/s. In the simulation we assumed that the uniform flow is combined with a homogenous isotropic turbulence. The assumption is made because the homogenous isotropic turbulence is the most easily characterised and is well defined in the literature. Considering the root mean square (rms) velocity fluctuations;

$$u' = \sqrt{\overline{u^2}}, v' = \sqrt{\overline{v^2}}, w' = \sqrt{\overline{w^2}}, \quad (13)$$

where u, v and w denote the vector components of the velocity fluctuation along the x, y and z axis in the Cartier coordinate system. According to the definition of homogeneous and isotropic turbulence [18]

$$u' = v' = w', \quad (14)$$

and u', v' and w' should not change over the entire turbulent field.

In the simulation, the turbulence length scale is assumed to be sufficiently small that the turbulence is assumed to be correlated at every point of interest on the calculation grid. In order to simplify the simulation, the instantaneous value of the velocity fluctuation on each point is assumed to be equal to the rms value, while the instantaneous direction of the velocity fluctuation on each point is independent. Let $T = [t_1, t_2 \dots t_n \dots t_m]$ denotes the period of time, in the flow field, for each point of interest $[x_i, z_j]$ on the x-z plane, the direction of the velocity fluctuations can be randomly set to be $D_{ij} = [D_{ij1}, D_{ij2} \dots D_{ijn} \dots D_{ijm}]$, where D_{ij} belongs to the uniform distribution, and $\sum D_{ij} = 0, D_{ijn} \in (-\pi, \pi)$. As the turbulence intensity varies in different outdoor environments, the velocity fluctuations and thus turbulence intensities are studied from 1% to 20% of the uniform flow. In this paper, the simulation results of 1% and 5% are presented. From Fig. 7, it can be seen that when the velocity fluctuation is relatively small, the envelope of the pressure field is recognisable. However, as the velocity fluctuation is increased to a certain level, the sound pressure field of the element becomes unpredictable.

B. Impact of an Airflow on an Airborne Ultrasonic Phased Array

Fig. 8 (a) presents predictions of the model for the peak-to-peak amplitude distribution of the sound pressure in air for an ultrasonic phased array formed by 8 circular elements. The diameters of the elements are 2mm, the distance between the centres of two neighbouring elements (pitch) is 3.5mm and the driving frequency of the array is 200 kHz. The expected focusing location is set to be x=0mm, y=0mm, z=60mm. From Fig. 8 (a), it can be seen that the actual focal point is located at x=0mm, y=0mm, z=48mm. This is because in the process of calculating the time delays among the elements, all elements are considered as point ultrasound sources, while the effects of their area are ignored. Neild et al. proposed that one possible solution to reduce such error is to increase the number of elements [10]. The simulation result of this study shows that increasing the distance between the neighbouring elements can also reduce this error, however the amplitude of the main lobe will be decreased and the amplitude of the grating lobes will be increased. Fig. 8 (b) presents the pressure field of a similar array, whose pitch is increased to 4.5mm. The actual location of

the focal point of the array is at x=0mm, y=0mm, z=55mm.

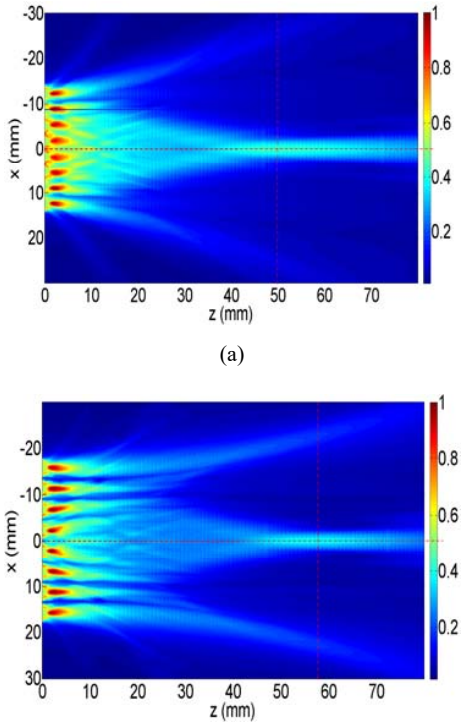

Fig. 8 Predicted peak-to-peak linear sound pressure field normalised to the max pressure in the field in air from (a) an array formed by 8 circular elements whose diameters are 2mm, pitches are 3.5mm and driven by a 200 kHz signal; (b) an array formed by 8 circular elements whose diameters are 2mm, pitches are 4.5mm and driven by a 200 kHz signal

Fig. 9 shows the pressure distribution of the same acoustic array presented in Fig. 8 (a), but influenced by uniform airflows. The airflows are directed along the positive direction of the x axis, and the speeds are 10m/s and 20m/s respectively. Similar to the impact on a single element, the impact of the uniform airflows along the vertical direction of the emitting signal on an acoustic array is mainly reflected in the modification of the steering angle of the array. Fig. 10 illustrates the predictions of the acoustic pressure field from the same array, influenced by a combination of uniform flow and homogeneous isotropic turbulent flows, as represented in Fig 7 (b). In Fig. 10 (a), it can be seen that even though the main direction of the flow is in the positive direction of the x axis, the actual location of the focal point is shifted in the negative direction of the x axis. In addition, the array is no long in as sharp a focus. Moreover, as shown in Fig. 10 (b), if the velocity fluctuation reaches a certain level, the array may be failed to be focused. In comparison to uniform flows, turbulent flows have more serious influence on airborne acoustic imaging, which may result the degradation of the acoustic images obtained by the array. Further investigations will be conducted to validate this deduction.

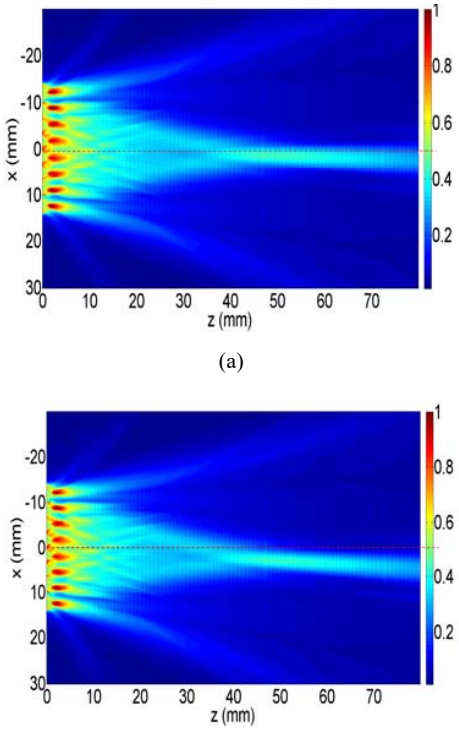

Fig. 9 Predicted peak-to-peak linear sound pressure field normalised to the max pressure in air from an array formed by 8 circular elements whose diameters are 2mm, pitches are 3.5mm and driven by a 200 kHz signal, impacted by a uniform airflow flowing along the positive direction of the x axis at a speed of 10 m/s (a) and 20 m/s (b)

IV. Conclusions

In this paper, a model for sound pressure fields from a single ultrasound element or an ultrasonic phased array impacted by airflows is presented. The model can be used to determine the actual focused sound filed location of an array exposed in a known flow field. From the presented simulation results based upon this model, it can be concluded that uniform flows in the direction orthogonal to the acoustic propagation have a noticeable influence on the sound pressure field, which is reflected in the twisting of the steering angle of the array. Uniform flows in the same direction as the acoustic propagation have negligible influence on the array. For an array impacted by a turbulent flow, determining the location of the focused sound field becomes difficult due to the irregularity and continuously changing direction and the speed of the turbulent flow. In some circumstances, ultrasonic phased arrays impacted by turbulent flows may not be capable of producing a focused sound field.

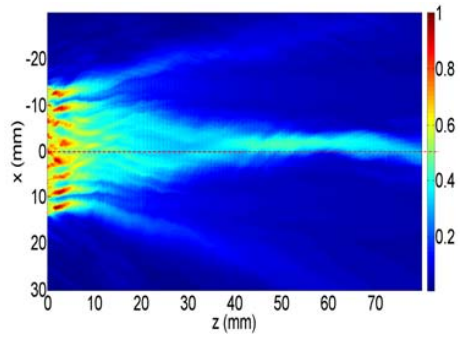

(a)

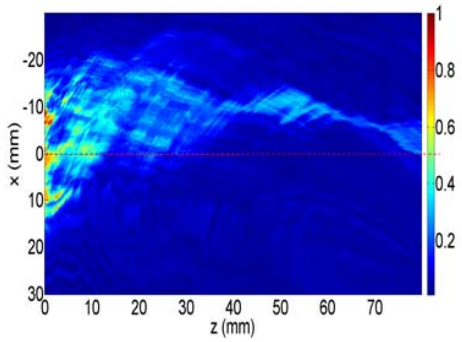

(b)

Fig. 10 Predicted peak-to-peak linear sound pressure field normalised to the max pressure in air from an array formed by 8 circular elements whose diameters are 2mm, pitches are 3.5mm and driven by a 200 kHz signal, impacted by a combination of uniform and homogeneous isotropic turbulent airflows. The uniform flow is flowing along the positive direction of the x axis at a speed of 5 m/s, and the velocity fluctuation of the turbulent flow is 1% (a) and 5% (b) of the uniform flow

REFERENCES

[1] Z. Zhang, S. Kodagoda, D. Ruiz, J. Katupitiya, and G. Dissanayake, "Classification of Bidens in Wheat Farms," *In Mechatronics and Machine Vision in Practice*, *15th International Conference on IEEE*, pp. 505-510, 2008.

[2] D. M. Bulanon, T. Kataoka, Y. Ota, and T. Hiroma, "AE—automation and emerging technologies: a segmentation algorithm for the automatic recognition of Fuji apples at harvest," *Biosystems Engineering*, vol. 83, no. 4, pp. 123-135, 2002.

[3] M. Dunn, J. Billingsley, and N. Finch, "Machine vision classification of animals," *In Mechatronics and Machine Vision 2003: Future Trends: Proceedings of the 10th Annual Conference on Mechatronics and Machine Vision in Practice,* Perth, Australia, pp. 9-11, 2003.

[4] D. Gao, T-F Lu, and S. Grainger, "A new method of feature extraction and location derivation in vineyards using point clouds," *Applied Engineering in Agriculture*, vol. 30, no. 2, pp. 293-306, 2014.

[5] A. J. Fenn, D. H. Temme, W. P. Delaney, and W. E. Courtney, "The development of phased-array radar technology," *Lincoln Laboratory Journal*, vol. 12, no. 2, pp. 321-340, 2000.

[6] W. N.Christiansen, & J. A. Högbom, *Radiotelescopes*. CUP Archive, 1987.

[7] R. A. Monzingo, and T. W. Miller, *Introduction to adaptive arrays*, SciTech Publishing, 1980.

[8] M. D Zoltowski, and A. S. Gecan, "Advanced adaptive null steering concepts for GPS," *In Military Communications Conference*, *IEEE*, vol. 3, pp. 1214-1218, November, 1995.

[9] S. C. Wooh, and Y. Shi, "Influence of phased array element size on beam steering behaviour," *Ultrasonics*, vol. 36, no. 6, pp. 737-749, 1998.

[10] L. G. Ullate, and J. L. San Emeterio, "A new algorithm to calculate the transient near-field of ultrasonic phased arrays," *Ultrasonics, Ferroelectrics, and Frequency Control, IEEE Transactions on*, vol. 39, no. 6, pp. 745-753, 1992.

[11] A. Neild, D. A Hutchins, T. J. Robertson, L. A. J. Davis, and D. R. Billson, "The radiated fields of focussing air-coupled ultrasonic phased arrays," *Ultrasonics*, vol. 43, no. 3, pp. 183-195, 2005.

[12] L. Azar, Y. Shi, and S. C. Wooh, "Beam focusing behavior of linear phased arrays," *NDT & E International*, vol. 33, no. 3, pp. 189-198, 2000.

[13] W. S. H. Munro, and C. Wykes, "Arrays for airborne 100 kHz ultrasound," *Ultrasonics*, vol. 32, no. 1, pp. 57-64, 1994.

[14] M. Moebus, and A. M. Zoubir, "Three-dimensional ultrasound imaging in air using a 2D array on a fixed platform," I*n Acoustics, Speech and Signal Processing, IEEE International Conference on,* vol. 2, pp. II-961, April, 2007.

[15] J. M. Noble, and H. J. Auvermann, "The Effects of Large and Small Scale Turbulence on Sound Propagation in the Atmosphere," *Army Research Lab White Sands Missile Range NM*, no. ARL-TR-565, 1995.

[16] L. Jakevičius, and A. Demčenko, "Ultrasound attenuation dependence on air temperature in closed chambers," *Ultragarsas (Ultrasound)*, vol. 63, no. 1, pp. 18-22, 2008.

[17] T. Yang, K. Nadimpalli, and B. Cechet, "Local wind assessment in Australia: Computation methodology for wind multipliers," *Geoscience Australia*, viewed 15 September 2015, Retrieved from http://www.ga.gov.au/corporate_data/75299/Rec2014_033.pdf.

[18] P. Sagaut, and C. Cambon, *Homogeneous turbulence dynamics*, Cambridge University Press, 2008.